Distribution of luminescent centers in Ce^{3+}-ion doped amorphous stoichiometric glass $BaO–2SiO_2$ and dedicated glass ceramics

M.V. Korjik[a,*], A. Vaitkevicius[b], D. Dobrovolskas[b], E.V. Tret'yak[c], E. Trusova[d], G. Tamulaitis[b]

[a] *Research Institute for Nuclear Problems of the BSU, 220030, Minsk, Belarus*
[b] *Semiconductor Physics Department and Institute of Applied Research, Vilnius University, Sauletekio 9-III, LT-10222 Vilnius, Lithuania*
[c] *Research Institute for Physical Chemical Problems of the BSU, 220080, Minsk, Belarus*
[d] *Belarusian State Technological University, 13a Sverdlova str., 220006, Minsk,Belarus*

Abstract

We investigated the influence of crystallization conditions on the luminescent properties of Ce^{3+}-ions doped stoichiometric glass $BaO–2SiO_2$ at the different stages of its transformation from amorphous phase to glass ceramics. The samples were investigated by confocal luminescence spectroscopy. It was found that the luminescent properties of the cerium-doped glass and the glassceramics composite consisting of $BaSi_2O_5$ crystallites and residual glass are quite similar, though the luminescence band in the composites are slightly redshifted and narrower.

Keywords: glasses, glass-ceramics, luminescence

1. Introducion

There is a strong demand for development of new inorganic luminescent materials which nowadays shows tremendous progress through nano-engenering of the materials. Particularly, the last decade evidenced an impressive progress in the lighting technology based on the light emitting diodes (LED). The construction of the white LEDs is rather simple: the blue LED is

*Corresponding author
Email address: Mikhail.Korjik@cern.ch (M.V. Korjik)

encapsulated in a transparent material containing phosphor material YAG:Ce emitting yellow Photo Luminescence (PL). The combination of the two spectral components results in the spectrum accepted as a white light. However, to improve the color rendering of the white LED emission, more phosphors are necessary to be used however, not many phosphors are suitable to operate at blue light excitation. The shift of the excitation to the near UV (360-390 nm) increases the amount of the compounds and activating ions suitable for creation new phosphors for the LED based lighting.

Among variety of inorganic materials silicates are seems to be prospective to construct new phosphors. They find numerous application as luminescent materials in a crystalline phase. The rare earth (RE) containing single-crystalline oxy-ortho RE_2SiO_5 and pirochlor $RE_2Si_2O_7$ silicates doped with Ce are good scintillation materials [1]. Most of the silicate crystalline materials while doped with Ce, possess blue luminescence band at near UV excitation, what is a bottleneck that hinders their application for lighting.

In a glass form, silicates also possess several limitations, especially lower thermal conductivity and difficulty to stabilize activating ions in a needed valent state. For instance, pure SiO_2 does not allow an incorporation of RE-ions with reasonable concentration due to crystal-chemical reasons. Modification of the glass net with different additives, especially La, allows doping however, stabilization of needed valent state still remains the problem. Nevertheless, similar to single crystalline materials, some complicated silicate glasses show bright near UV or blue luminescence. For instance, lithium silicate glass is widely used for making of neutron sensitive scintillation sensors [2].

Glass ceramic materials possess several advantages combining the properties of crystals and glass, especially the high thermal conductivity. Their production is an industrial domain which promotes future development of the materials since sixties [3]. However, at the development of luminescent glass ceramics materials several matters still have to be answered. One of them is a transformation of the luminescent properties at the material crystallization. Dissordering is replaced by ordering in a crystallized part of the material, so crystalline field, distribution of the local charge compensation in the vicinity of activator as well, are changed. For instance, recent study of europium doped barium disilicate glass system showed that luminescent properties of the material are strongly affected by crystallization [4, 5]. Eu^{2+}-ions luminescence, which was not detected in a mother glass, became dominating when glass material was crystallized by thermal treatment. It was suggested that Eu^{3+}-ions delivering the red luminescence are preferably localized in

the amorphous glass, while the Eu^{2+}-ions emitting in the blue-green region become dominating after partial crystallization of the glass. The results published in [6] showed that the significant amount of Eu^{3+}-ions is always present in fluorzirconate based glass ceramics reducing the performance of these materials as both scintillators and storage phosphors. Besides Eu luminescence, strong UV luminescent band was observed in bariumdisilicate phosphore at the doping with Pb ions [7]. However, Ce^{3+}-ions luminescence is not studied well in this material.

In our study we considered an effect of crystallization on luminescent properties of Ce^{3+}-ions in barium disilicate glass system. The disilicate of barium is unique by its capability to be manufactured in several states: amorphous at the stoichiometric mixture $BaO–2SiO_2$ produced by the ordinary glass production technique, as glass-ceramics [8], and in a crystalline form. The $BaO–2SiO_2$ system exhibits homogeneous nucleation [9], and the size of the crystallites can be controlled by the glass annealing temperature.

Similar to europium, cerium is also heterovalent ion and stabilized in inorganic compounds in thre- to four-valent states [1]. Ce^{3+}-ions possesses bright interconfiguration *d-f* luminescence in many wide forbidden zone compounds. Ce^{4+}-ions does not show intrinsic luminescence properties however, it provides a wide unstructured absorption in UV range due to ligand-metal charge transfer transitions [10]. Large concentration of Ce^{4+}-ions in the material also provides a braunish color of the samples. To study the sensitivity of the resulting luminescence spectrum to the ratio between the crystallized and residual amorphous parts of the glass, we investigated the luminescence properties of cerium doped glass $BaO–2SiO_2$ and glass ceramics obtained from this glass at different temperature and duration of thermal treatment.

2. Materials and methods

2.1. Materials

Powders of $BaCO_3$ and SiO_2 with 99.99% purity were used. Powder of $Ce_2Si_2O_7$ were used as a source of Ce^{3+} ions. All the chemicals were produced by NeoChem (Russia).

2.2. $BaO–2SiO_2$ glass obtaining

Glass $BaO–2SiO_2$ was obtained by melting of mixture of 7.22 g. $BaCO_3$, 4.40 g. SiO_2 and 0.10 g. $Ce_2Si_2O_7$ (1 wt. %. over the glass stoichiometry) in a aluminium oxide ceramic crucible in gas furnance (FALORNI) at

1450°C for 2 hours. To avoid crystallization during cooling and reducing the mechanical stresses in the samples, the glass was casted on a non-preheated steel block and subsequently treated in a muffle furnace preheated to 700°C for 2 hours. The obtained glass block was transparent and colorless, indicate about preservation of cerium ions oxidation level. The glass was cutted into plates with thickness of 1 mm, that then were annealed on air at 850°C for 30 min and 900°C for 15 min (crystallization of $BaSi_2O_5$ monoclinic symmetry occurs at $\sim$ 880°C [8]). The heating rate of the furnace was 50°C/min. Transparent and colorless glass at first after thermal treatment at 850°C became opaque and after heat treatment at 900°C – lactescence. After heat treatment, all samples remained colorless.

2.3. Characterization

To observe an effect of crystallization on luminescent properties of the samples we investigated parameters of luminescent band at macro- and micro-level of the material. It allowed to observe a possible influence of samples structure ordering on the PL band. The PL mapping was performed using the microscope *WITec Alpha* 300 S in the confocal mode. An objective with the numerical aperture NA = 0.6 was used ensuring the lateral spatial resolution of $\sim$250 nm and axial resolution of $\sim$1.6 μm. The microscope was coupled via optical fiber with a spectrometer followed by a thermoelectrically cooled CCD camera. A violet laser diode (ALPHALAS) emitting at 405 nm was used in spatially-resolved photoluminescence spectroscopy experiments.

Mother glass and annealed samples were milled before infrared absorption (IR) spectra measurements. The IR spectra of the powdered samples were collected in 400–4000 cm^{-1} wave number ranges using the Thermo Nicolet Avatar FTIR–330 spectrometer at room temperature by diffuse reflectance method.

3. Results

The glass BaO-2SiO_2 doped with Ce^{3+} ions demonstrates bright inter-configuration *d-f* luminescence in a blue-green spectral range at room temperature. The excitation spectra include a strong band with maximum in the vicinity of 360-370 nm. Excitation band long wavelength shoulder is expanded up to 410 nm. At excitation near 360 nm luminescence maximum is near 460 nm and the quantum yield of approximately 0.3 at excitation by 360 nm. At the excitation near 400 nm (Fig.1) luminescence maximum is

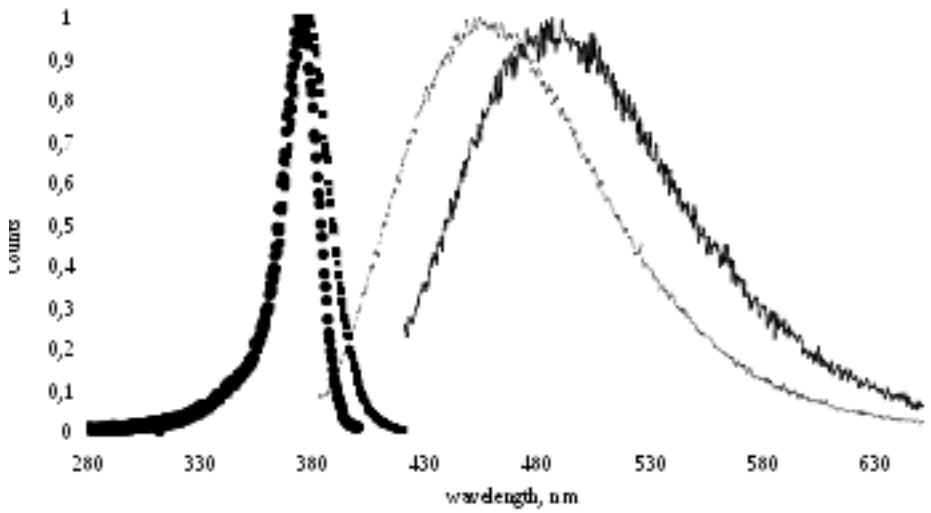

Figure 1: Spectra of luminescence at excitation 370 nm (dashed line) and 400 nm (full line) and luminescence excitation at registration 450 nm (squres) and 500 nm (circles) of mother glass sample measured at room temperature

shifted toward 490 nm. It indicates that Ce^{3+} ions occupies in the glass a variety of positions with slightly different surrounding.

The spectrally-integrated luminescence spectra of the samples under study are presented in Fig. 2. In spatially resolved experiments, we mapped areas of two sizes, 40×40 μm^2 and 90×90 μm^2, both with resolution of 200×200 points. The shape of the luminescence band and the center of the mass of the luminescence band to detect the possible formation of new bands or the transformations of the luminescence band were studied. The band width is a good indicator to observe the variations in emission properties due to the changes in the surrounding of the emitting ion that can be expected at the transition from amorphous to crystalline phase. We paid an especial attention to the changes near the macroscopic defects like bubbles or granules. The agglomeration of crystallites in the vicinity of the defects could be expected. This effect could cause the most substantial differences between luminescent properties in amorphous and crystalline phases. The luminescence parameters are summarized in Table 1.

The PL intensity in the sample annealed for 15 min at 900°C is approximately 40% weaker than that of the reference sample. In comparison, PL

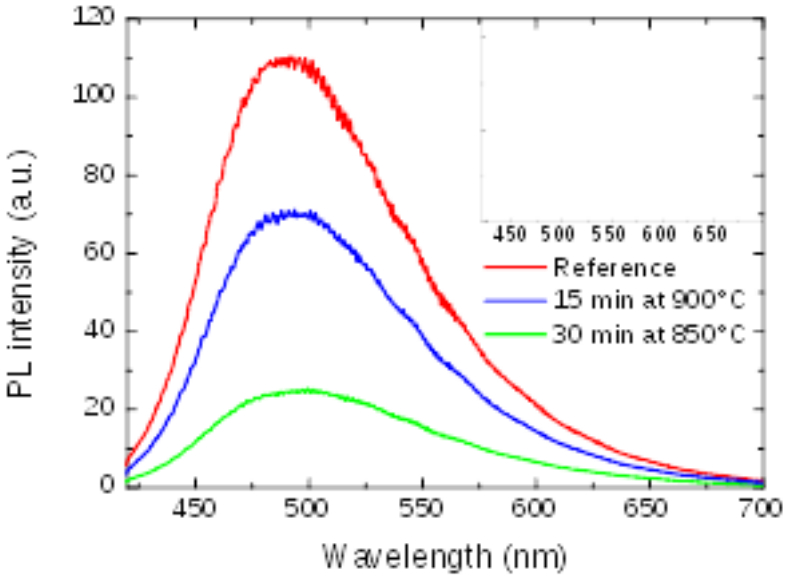

Figure 2: Photoluminescence (excitation at 405 nm) spectra of untreated reference Ce^{3+}-doped glass (red curve) and annealed glasses (conditions indicated) at room temperature. Inset shows normalized spectra

Table 1: Average values and standard deviations of PL parameters of the samples under study in the bulk of the glass 150 μm below the surface

	Untreated mother glass	Annealed at 900°C for 15 min	Annealed at 850°C for 30 min
Peak position, nm	490(6)	496(9)	500(9)
Spectral center of mass, nm	517(1)	522(2)	524(2)
FWHM, nm	111(3)	92(9)	95(7)

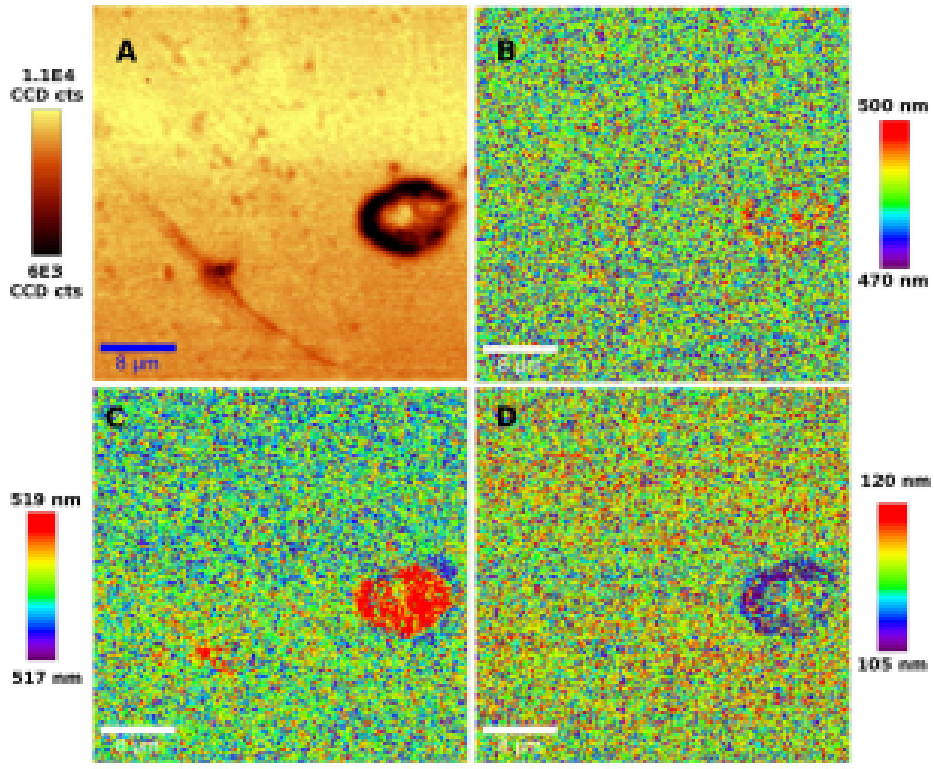

Figure 3: Spatial distribution of spectrally integrated photoluminescence intensity (upper left, A), band peak position (upper right, B), spectral center of mass (lower left, C), and band FWHM (lower right, D) on the surface of untreatedmother glass. A small scratch and pothole are visible

intensity of the sample annealed for 30 min at 850°C is approximately by a factor of 5 weaker than that of the reference sample. Probably, the different decrease in PL intensity is caused by decreased optical transmittance of samples due to partial crystallization of the samples. The PL band in the sample annealed for 30 min at 850°C is redshifted by ∼10 nm in respect to its position in the reference sample.

The spatial distribution of PL parameters is in general quite homogeneous. However, the glass contains at least two kinds of specific regions with distinctly different PL properties. The images presented in Fig. 3 encompass one of the typical features in the quite homogeneous background – an oval-shaped area with different PL properties. The area is 8-10 μm in diameter.In the PL intensity distribution (Fig. 3 A) it is noticeable as a non-uniform loop

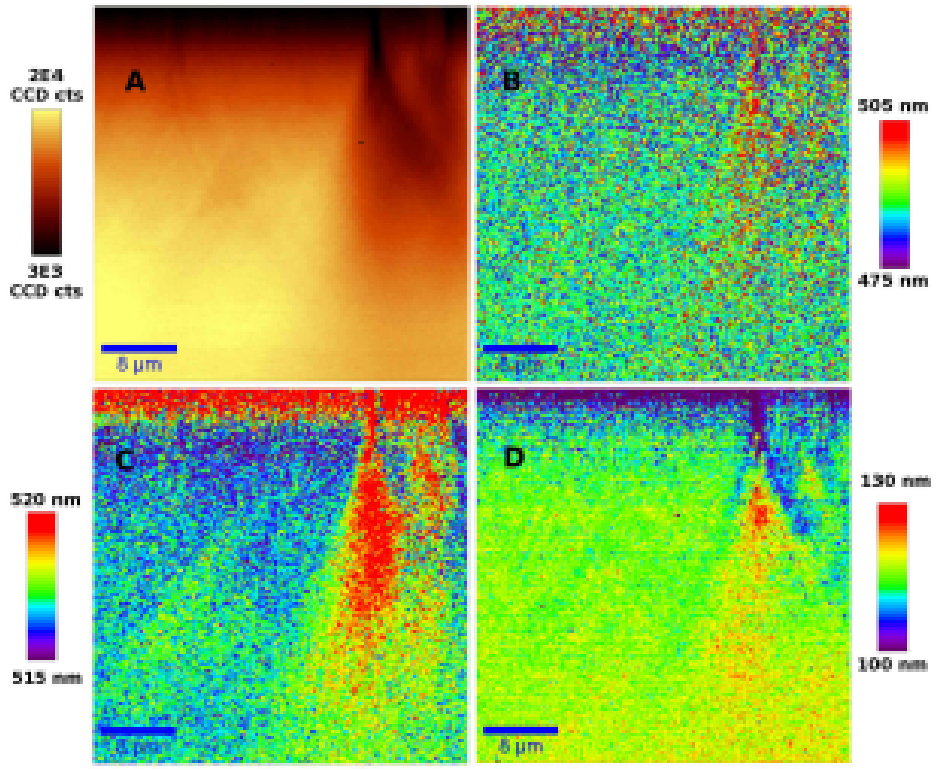

Figure 4: Mappings of spectrally integrated PLintensity (upper left, A), peakposition (upper left, B), spectral center of mass (lower left, C), and FWHM of the PL band (lower right, D) in the untreated motherglass with gnarls

of lower PL intensity.In the PL peak position (fig. 3B) andspectral center of mass (Fig. 3 B) mapping, a redshift of the PL band in this area is evident.The distinct area with lower PL intensity also exhibits a narrower band width (see the full width at half maximum in Fig. 3 D).

Mappings of the PL parameters distributions perpendicularly to the sample surface, across the oval shaped area, are presented in Fig. 4. These measurements reveal a column-like structure extending $\sim$30 μm into the sample.

Mappings of the PL parameters in the vicinity of the second typical distinct area are presented in Fig. 5. The area has the shape of a spherical bubble, roughly 27 μm in diameter.The region consists of a core, 15 μm in diameter, and a 6 μm thick shell. The PL intensity (Fig. 5 A) in the core is smaller than that in the background by a factor of 5.7. The PL intensity in the shell changes gradually.The PL band peak position (Fig. 5 B) is

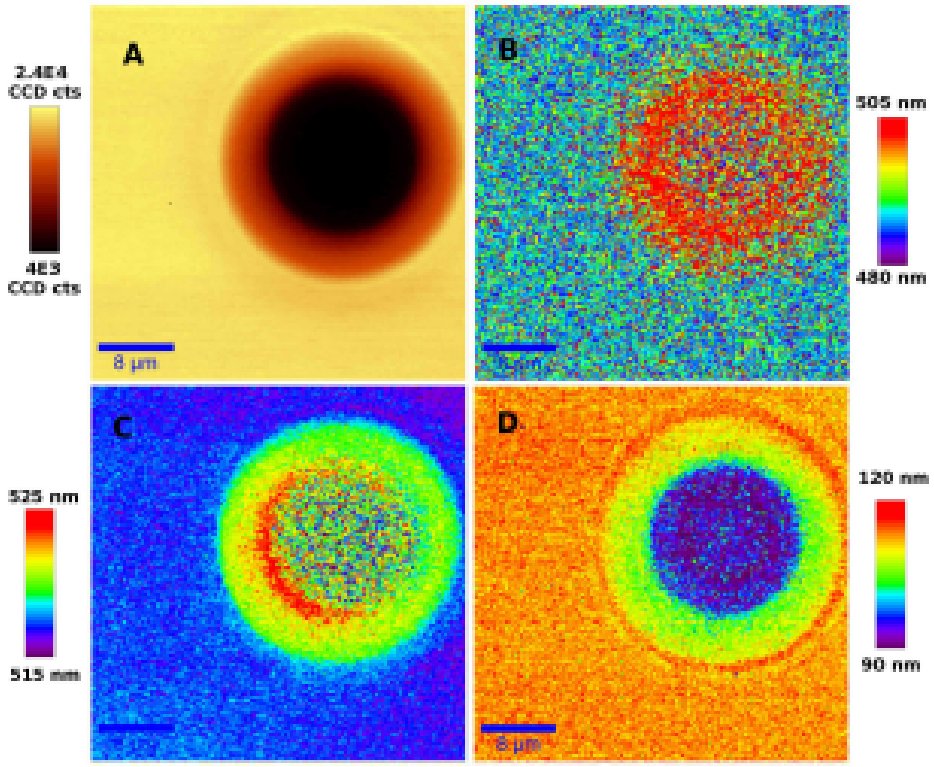

Figure 5: Mapping images of spectrally integrated PL intensity (upper, left), peak position (upper, left), spectral center of mass (lower, left) and FWHM (lower, right) of the PL band in the untreated mother glass with a bubble. The planar scan crosses the bubble

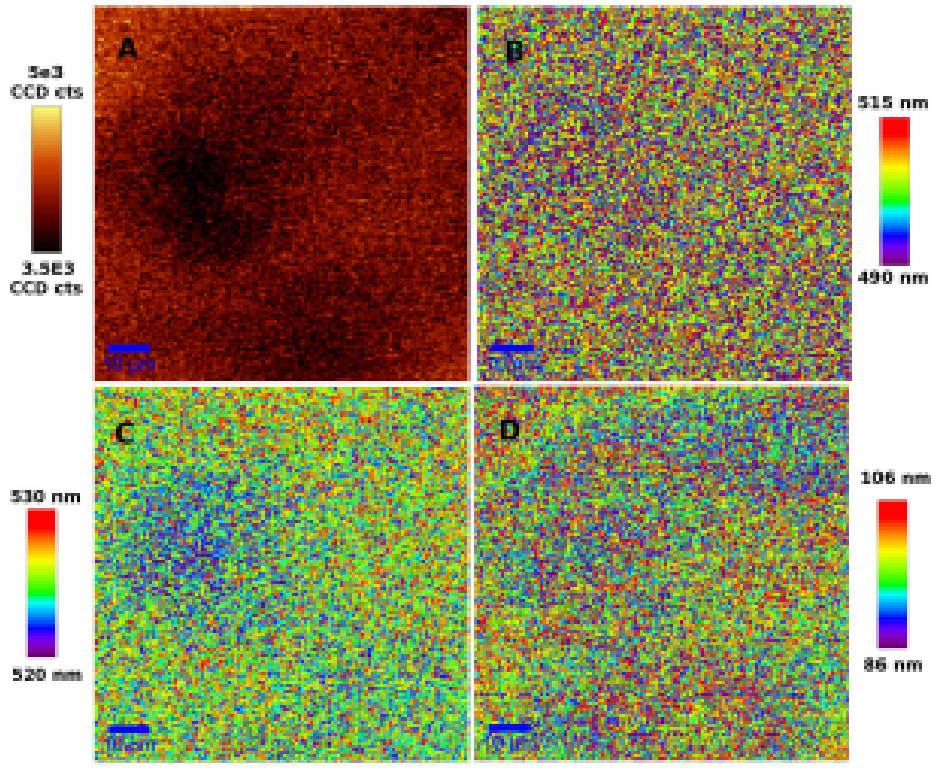

Figure 6: Mapping image of spectrally integrated photoluminescence intensity (upper left, A), band peak position (upper left, B), spectral center of mass (lower left, C), and FWHM (lower right, D) in the sample annealed at 850°C

redshifted, and the redshift is stronger in the shell. The red shift is more pronounced in the spectral center of mass mapping image (Fig. 5 C). The spatial distribution of FWHM is presented in Fig. 5 D). A considerable narrowing of the PL band is evidenced, especially in the core region.

After annealing, the sample remains predominantly homogeneous. The only influence of annealing on the spatial distribution of PL parameters was formation of regions of irregular shape where the PL intensity was lower than in the bulk of the sample by a factor of 1.1. This modification was observed for the samples subjected to annealing both at 850°C and 900°C.

The irregularly shaped regions are visible in the distributions of all parameters of the sample annealed at 850°C (see Fig. 6). The inhomogeneity was checked by calculating Pearsons correlation coefficients (R) for the pairs of PL parameters obtained by spatially-resolved PL spectroscopy. The PL

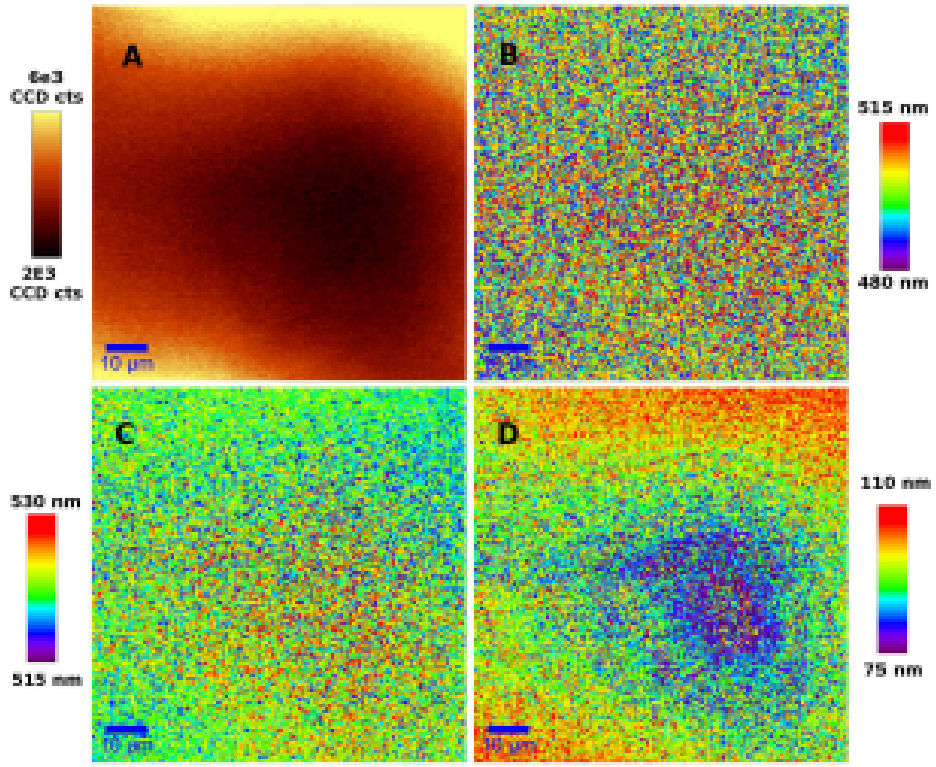

Figure 7: Mapping image of spectrally integrated photoluminescence intensity (upper left, A), band peak position (upper left, B), spectral center of mass (lower left, C), and FWHM (lower right, D) in the sample annealed at 900°C

intensity and the blue shift of the PL spectral center of mass (see Figures 6 A and C) is significant ($R = 0.4$). No significant correlation ($R < 0.3$) has been observed for other pairs of PL parameters in this sample.

Images of mapping the PL parameters in the sample annealed at 900°C are presented in Fig. 7. Strong correlation ($R = 0.6$) between PL intensity (Fig. 7 A) and FWHM of the PL band (Fig. 7 D) is evident. No significant correlation ($R < 0.3$) has been observed for other pairs of PL parameters.

4. Discussions

To justify an origin of minor Ce^{3+} luminescence band changes due to annealing we measured infrared (IR) transmittance spectra of mother glass and annealed samples. Fig. 8 shows IR spectra measured in the range 2000-

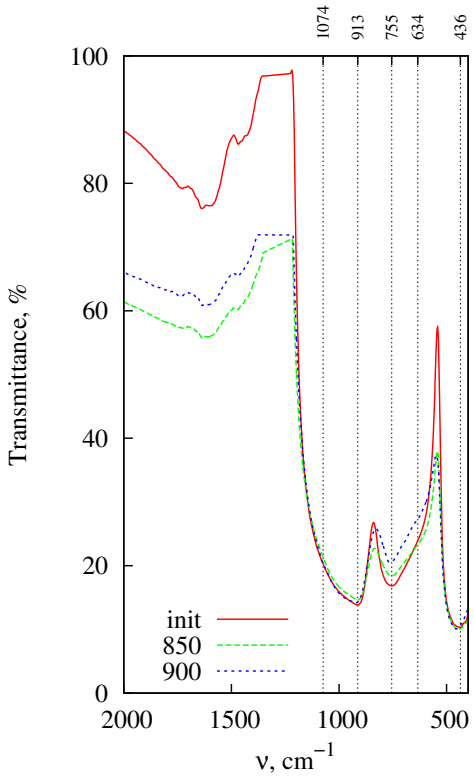

Figure 8: IR spectra of mother glass (init) and glasses annealed at 850°C (850) and 900°C (900) for 30 and 15 min respectively

400 cm^{-1}. Several characteristic bands dedicated to silicate systems were measured [11, 12]. It is seen that crystallization of the mother glass does not affect characteristic peaks in the vicinity of 430 and 900 cm^{-1}. However, absorption band peaked at 755 cm^{-1} shows decreasing of intensity whereas band intensity near 634 cm^{-1} increases. It is in a good agreement with the fact that an amount of ring structures is decreased in partially crystallized glass. The band at 635 cm^{-1} shows growth due to the increased role of interaction through bridging oxygen with creation of junctions of type Si—O–Si between groups of the type ≡Si–O and –SiO_3. Thus, we supposed that crystallization in glass obtained from stoichiometric composition does not change dramatically vibration modes. Due to this reason no sufficient change of the configuration potential of the Ce^{3+} emitting level is expected.

The parameters of observed luminescence bands measured in the mother glass and treated samples are summarized in in Table 1. To avoid any influence off the sample surface, the parameters were calculated using the PL spectra measured in the glass bulk 150 μm below the surface. They show that annealing of the glass imposes a red shift of the PL band. For both peak position and center of mass the red shift is larger in the sample annealed at 850°C for 30 min. than that in the sample annealed at a higher temperature (900°C) but for a shorter period (15 min). The standard deviation of both parameters increases after annealing from 6 nm to 9 nm for PL peak position and from 1 nm to 2 nm for spectral center of mass. The average PL band width decreases after annealing, and the standard deviation increases.

The increase of the standard deviation for all PL parameters is an indication of decreased homogeneity in the annealed samples, possibly, due to their partial crystallization.The decrease by 20% of the luminescence band width due to annealing can be interpreted by ordering of the crystalline field around the activator ions in the crystallites. Meanwhile, the relatively small spectral shift of the luminescence band peak position and spectral center of mass evidence that the glass transformation to crystalline phase proceeds without changing the Ce^{3+} ion positions in the matrix. Thus, the ordering of the structure during crystallization of $BaO–2SiO_2$ system occurs due to the change of the anion-cation distances without strong rearrangement of the net. We consider this effect to be an evident advantage of stoichiometric compositions. The spectral features of not annealed glass presented in Figs. 2-4 show that some nucleation of around defects occurs already in the mother glass. The luminescence band in the vicinity of the defects is redshifted and the FWHM is smaller. However, these changes are relatively small and do not make any significant influence on the average values.

5. Conclusion

In conclusion, crystallization of $BaO–2SiO_2$ system doped with Ce^{3+} ions results only in small changes of the luminescence parameters. Observed feature is favorable for application of this glass system as phosphor material with low sensitivity of spectral parameters to fabrication conditions resulting in various glass/to ceramics ratios in the final product. That the cerium-doped $BaO–2SiO_2$ glasses might be suitable to produce high luminosity phosphors under excitation in UV to violet spectral region.

References

[1] P. Lecoq, A. Annenkov, A. Gektin, M. Korzhik, C. Pedrini, Inorganic Scintillators for Detector Systems: Physical Principles and Crystal Engineering, Particle Acceleration and Detection, Springer Berlin Heidelberg, 2006.

[2] A. Spowart, Neutron scintillating glasses: Part 1: Activation by external charged particles and thermal neutrons, Nuclear Instruments and Methods 135 (3) (1976) 441 – 453. doi:http://dx.doi.org/10.1016/0029-554X(76)90057-4.

[3] P. W. McMillan, Glass-ceramics,, Academic Press, London; New York, 1964.

[4] J. H. Park, J. S. Kim, J. T. Kim, Luminescent Properties of $BaSi_2O_5$:Eu^{2+} Phosphor Film Fabricated by Spin-Coating of Ba-Eu Precursor on SiO_2 Glass, Journal of the Optical Society of Korea 18 (1) (2014) 45–49. doi:10.3807/JOSK.2014.18.1.045.

[5] A. Herrmann, A. Simon, C. Rssel, Preparation and luminescence properties of eu2+-doped basi2o5 glass-ceramics, Journal of Luminescence 132 (1) (2012) 215–219. doi:http://dx.doi.org/10.1016/j.jlumin.2011.08.024.

[6] B. Henke, C. Palick, P. Keil, J. A. Johnson, S. Schweizer, Eu oxidation state in fluorozirconate-based glass ceramics, Journal of Applied Physics 106 (11) (2009) 113501–6. doi:http://dx.doi.org/10.1063/1.3259390.

[7] D. S. Thakare, S. K. Omanwar, P. L. Muthal, S. M. Dhopte, V. K. Kondawar, S. V. Moharil, Uv-emitting phosphors: synthesis, photoluminescence and applications, physica status solidi (a) 201 (3) (2004) 574–581. doi:10.1002/pssa.200306720.

[8] W. Holand, G. Beall, Glass Ceramic Technology, Wiley, 2012.

[9] Y. Takahashi, H. Masai, T. Fujiwara, Nucleation tendency and crystallizing phase in silicate glasses: A structural aspect, Applied Physics Letters 95 (7) (2009) 071904–3. doi:http://dx.doi.org/10.1063/1.3206931.

[10] D. Pauwels, N. Le Masson, B. Viana, A. Kahn-Harari, E. van Loef, P. Dorenbos, C. van Eijk, A novel inorganic scintillator: Lu2si2o7 :ce3+ (lps), Nuclear Science, IEEE Transactions on 47 (6) (2000) 1787–1790. doi:10.1109/23.914446.

[11] K. Rao, Structural Chemistry of Glasses, Elsevier Science Ltd, Oxford, 2002.
URL http://www.sciencedirect.com/science/book/9780080439587

[12] P. McMillan, Structural studies of silicate glasses and meltsapplications and limitations of raman spectroscopy, American Mineralogist 69 (7–8) (1984) 622–644.